PROCEEDINGS OF SCIENCE

Charm spectroscopy from amplitude analyses in $B_{(s)}$ decays at LHCb

Melissa Maria Cruz Torres[a,*]

[a] *Universidad Nacional Autónoma de Honduras, Blv Suyapa, Honduras*

E-mail: melissa.maria.cruz.torres@cern.ch/melissa.cruz@unah.edu.hn

Amplitude analysis of B mesons decays offer a good laboratory for charm spectroscopy studies. Theoretical and experimental models of Quantum Chromodynamics can be tested. This provides the opportunity to gain a better understanding of the underlying dynamics of charm mesons which can give rise to other interesting phenomena. Several analyses performed by the LHCb experiment that gather new insight into charm spectroscopy are presented in this document.

10th International Workshop on Charm Physics (CHARM2020), 31 May - 4 June, 2021 Mexico City, Mexico - Online

*Speaker

PoS(CHARM2020)011

1. Observation of a new excited D_s^+ meson in $B^0 \to D^- D^+ K^+ \pi^-$ decays

The study of charm meson spectroscopy offers a unique place for testing theoretical and experimental Quantum Chromodynamics (QCD) models. Particularly, the charm-strange spectrum is rich in structures allowing to search for predicted resonant states and to test proposed theories [1, 2]. Some charm-strange states are experimentally well established [3] like the two $1S$ meson and four $1P$ states, but there are some others that still have not been observed, namely

- The 2^1S_0 state, which is predicted as the radial excitation of the pseudoscalar D_s^+ state; the lightest with mass around 2.6 GeV.
- Two D-wave states: $1^3D_2(2^-)$ and $1^1D_2(2^-)$, with mass around 2.86 GeV.
- Three P-wave states: $2^3P_0(0^+)$, $2^1P_1(1^+)$ and $2^3P_2(2^+)$ with mass around 3 GeV.

This nomenclature refers to the meson state - $n^{2S+1}L_j$, being n the principal quantum number, L the orbital angular momentum and S the spin. Spin-parity is denoted as J^P.

A privileged place to search for charm-strange mesons and to measure their properties is provided by the study of B-decays. The B mesons decays are usually characterized by having well defined initial state and low background levels. One, of the still missing charm-strange resonance, as indicated above, is the the radial excitation of the pseudoscalar ground-state D_s^+ meson 2^1S_0. Studies have been conducted to D_s states decaying to the DK pair, thus, only sensitive to D_s natural spin-parity states. A scenario that have not been explored, is the study of D_s^+ resonances decaying to $D^+K^+\pi^-$ from B decays. The advantage of of this process is that all spin-parity D_s states in a large mass range can be accessed. Moreover, if the $K\pi$ system of the $D^+K^+\pi^-$ decay is restricted to low mass values (below of the $K^*(892)^0$ threshold) then only D_s^+ resonances with unnatural spin-parity ($J^P = 0^-, 1^+, 2^-, ...$) can decay in $DK\pi$. This allows the possibility to search for the missing $D_s(2S)$ state, with mass around 2.6 GeV and $j^P = 0^-$.

In this analysis the observation of a new excited D_s^+ state in the $D^+K^+\pi^-$ spectrum is reported. The strategy consisted in performing an amplitude analysis of the $B^0 \to D^-D^+K^+\pi^-$ decays, with the restriction of the $K\pi$ mass lying below 0.75 GeV, indicated as the low $K^+\pi^-$ mass region. To this purpose, the data collected by the LHCb experiment from 2016 to 2018, representing an integrated luminosity of 5.4 fb^{-1} from pp collision at 13 TeV in the centre-of-mass energy is used. The amplitude analysis was performed using the helicity formalism.

After a selection criteria based on the topology and kinematics of the decay is applied, the signal and reminiscent background distributions are parametrized. The signal distribution is modeled using the sum of two Crystal Ball [4] and the background accordingly with an exponential function. Then, an unbinned maximum-likelihood fit is performed to the mass distribution of B^0 candidates, with the $K^+\pi^-$ mass restricted to low values. A total of 444 ± 27 signal candidates was extracted [5].

The data distribution with the fit results overlaid is shown in Fig. 1. The projection of B^0 candidates within a signal window of $\pm$ 20 MeV around the B^0 mass, in the D^+D^- versus $D^+K^+\pi^-$ squared mass is shown in Fig. 2. In this Dalitz plot, clearly can be seen a cluster of events in the $D^+K^+\pi^-$ mass around 2.6 GeV. This structure has not been observed before. A small peak at the $D^+K^+\pi^-$ threshold corresponds to $Ds1(2536)^+$ state. In the D^+D^- system no resonant is noticed.

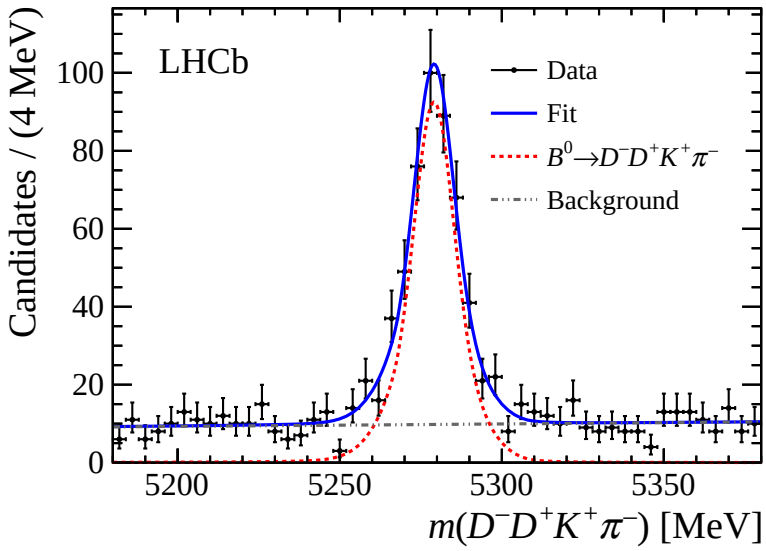

Figure 1: Data distribution in the B^0 spectrum with the $K^+\pi^-$ mass restricted to low values. The fit results are overlaid and shown in blue.

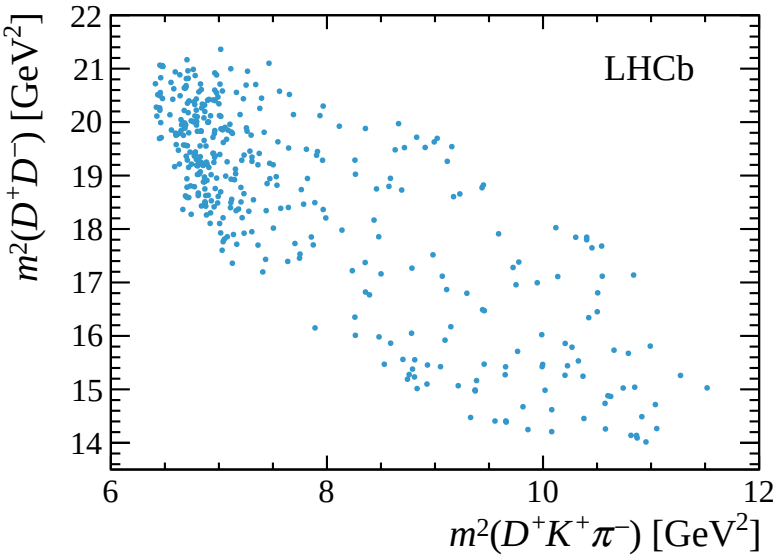

Figure 2: Dalitz plot in the D^+D^- and $D^+K^+\pi^-$ systems. The B^0 candidates are required to fall within 20 MeV in the signal window.

The amplitude analysis is required to study the structures present in the $D^+K^+\pi^-$ system. For the composition of the total amplitude, three D_s^+ components with unnatural spin-parity are considered:

- A new D_{sJ}^+ state at 2.6 GeV (three hypothesis: 0^-, 1^+.and 2^+)

- The $J^P = 1^+ D_{s1}(2536)^+$ state.
- A $J^P = 0^-$ non resonant (NR) component.

For the $K^+\pi^-$ system, the line shape is modeled by $J^P = 0^+ K_0^*(700)^0$ state for all three D_s^+ components. The line shapes of D_{sJ}^+, $D_{s1}(2536)^+$ and $K_0^*(700)^0$ are described by relativistic Breit-Wigner (BW) functions. The best fit quality was obtained when the D_{sJ}^+ spin parity hypothesis, $J^P = 0^-$, was evaluated. This state is denoted $D_{s0}(2590)^+$ and the measured pole mass and width is found to be $m = 2591 \pm 6 \pm 7$ MeV and $\Gamma = 89 \pm 16 \pm 12$ MeV, respectively. The first uncertainty represents the statistical error and the second due to systematic effects.

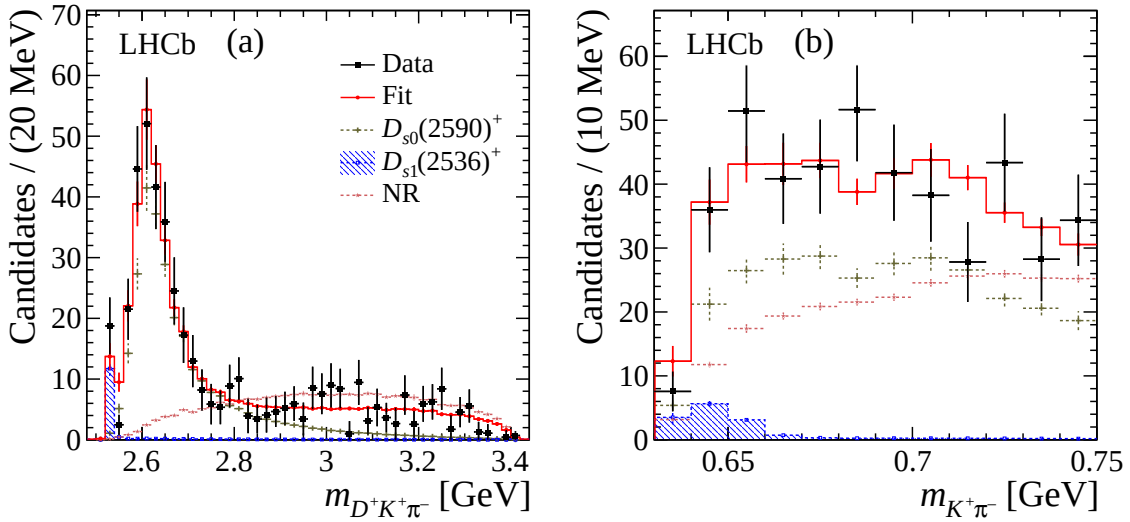

Figure 3: Dalitz plot fit results projections.

The Dalitz plot fit results [5] projected in each system are shown in Fig 3. From the $D^+K^+\pi^-$ distribution in Figure 3, a clear excess of event around 2.6 GeV can be seen. The projection of the cosine of the helicity angle ,θ_{Ds}, for the different spin parity hypotheses can be seen in Fig 4, where θ_{Ds} refers to the angle between the direction of the D^+ momentum and the opposite of the B^0 momentum. From here, indeed, can be concluded that the best parametrization is obtained with $J^P = 0^-$.

	Fit fraction ($\times 10^{-2}$)
$D_{s0}(2590)^+$	63 ± 9 (stat) ± 9 (syst)
$D_{s1}(2536)^+$	3.9 ± 1.4 (stat) ± 0.8 (syst)
NR	51 ± 11 (stat) ± 19 (syst)
D_{s0}^+ –NR	-18 ± 18 (stat) ± 24 (syst)
D_{s1}^+ / D_{s0}^+	6.1 ± 2.4 (stat) ± 1.4 (syst)

Table 1: Fit fractions contributions for the three D_s^+ components in the low $K^+\pi^-$ mass region. The interference fraction between $D_{s0}(2590)^+$ and NR is denoted as $D_{s0}^+ - NR$.

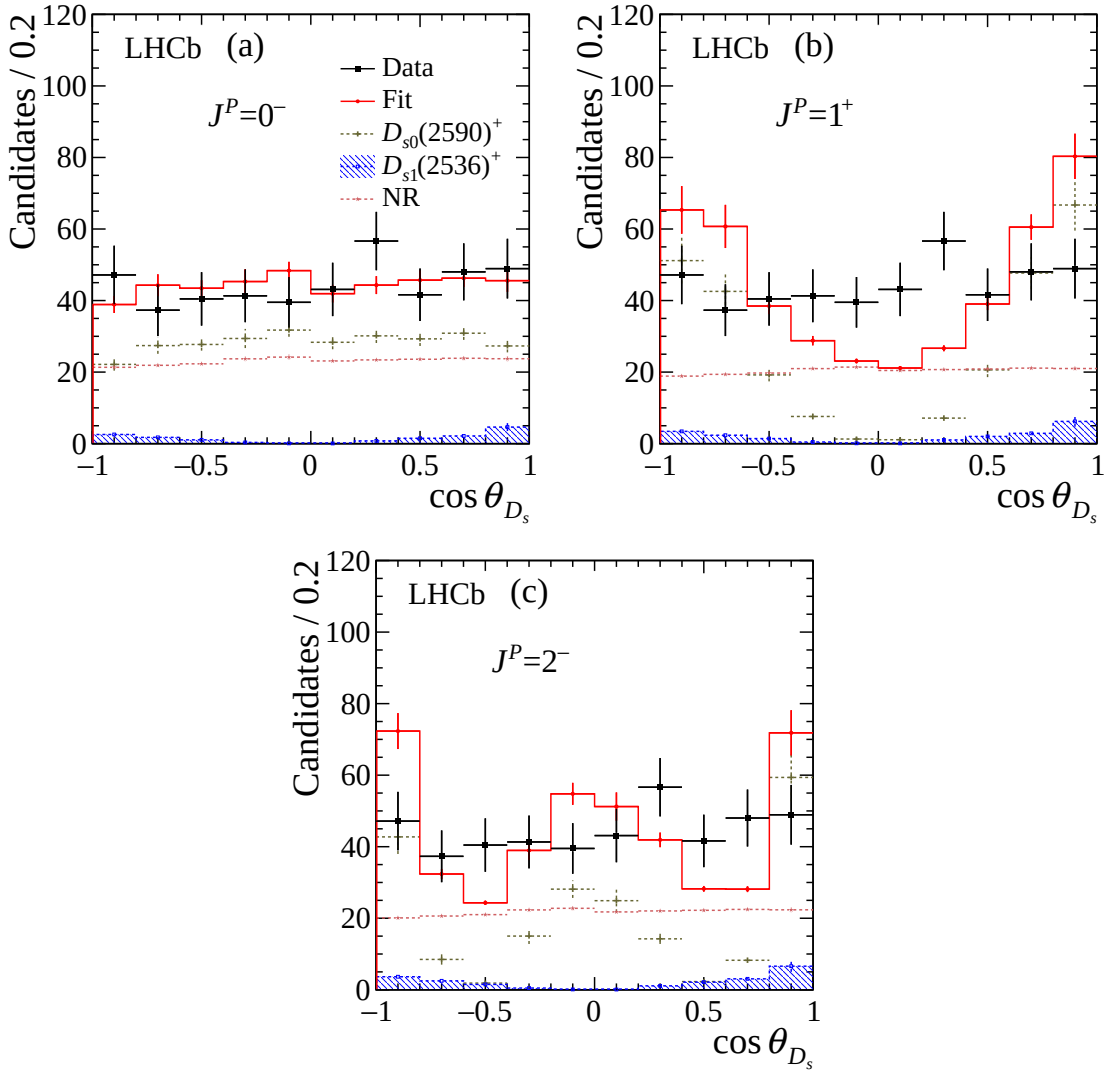

Figure 4: Dalitz plot in the D^+D^- and $D^+K^+\pi^-$ systems. The B^0 candidates are required to fall within ±20 MeV in the signal window.

Parameters results are summarized in Table 1 with the fit fraction contribution for each component indicated. In conclusion, a new excite D_s^+ meson is observed with a large statistical significance in the $D^-D^+K^+\pi^-$ system of the $B^0 \to D^-D^+K^+\pi^-$ decays.

2. Determination of quantum numbers for several excited charmed mesons observed in $B^- \to D^{*+}\pi^-\pi^-$

In this analysis, the potentiality of the decay channel $B^- \to D^{*+}\pi^-\pi^-$ to search for new charmed states and to determine of resonance parameters is exploited. For these purposes, several quasi-model-independent analysis and a four-body amplitude analysis are performed.

For example, the $D\pi$ system allows to search for natural spin-parity resonance $J^P = 0^+, 1^+, 2^+,...$, labeled as D^*. On the other hand, the study of $D^*\pi$ final states enables the possibility to study for both, natural and unnatural spin-parity resonances (except for $J^P = 0^+$). Therefore, the amplitude analysis of $B^- \to D^{*+}\pi^-\pi^-$ allows the full spin-parity analysis of charmed mesons. Particularly, the D_J spectroscopy in the $D^{*+}\pi^-$ system is explored.

The decay chain of this process can be understood as $B^- \to R^0\pi_2^-$, where $R^0 \to D^0\pi^+\pi_1^-$, being π_1^- and π_2^- the two identical pions in the final state. The dataset consists in the runI + run II data, corresponding to an integrated luminosity of $\mathcal{L} = 4.7$ fb^{-1} of pp collisions collected in the center-of-mass energies at 7 TeV and 13 TeV in the LHCb experiment. The extraction of the signal candidates correspond to 79120 events where 48.5% is from the run I dataset and 51.5% from run II [6]. Having two identical particles in the final state, the Dalitz plot is constructed on the symmetrical variables $m^2(D^{*+}\pi^-_{high})$ and $m^2(D^{*+}\pi^-_{low})$. The projection on these variables can be seen in Figures 5. The projection in the $m^2(D^{*+}\pi^-_{low})$ variable is shown in Fig. 6.

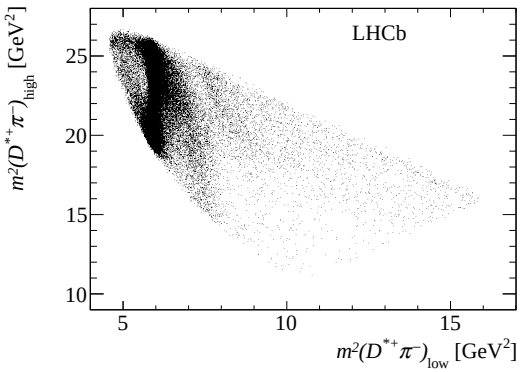

Figure 5: Projection of signal events in the $B^- \to D^{*+}\pi^-\pi^-$ Dalitz plot.

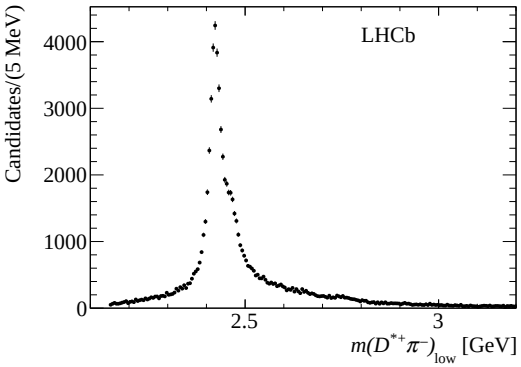

Figure 6: Projection of signal events in the $m^2(D^{*+}\pi^-_{low})$ system.

From Fig. 5, clear vertical bands can be seen around 5 GeV^2, this is understood as the presence of the well known $D_1(2420)$ and $D_2^*(2460)$ resonances. The existence of further weaker bands, at higher mass regions, is not so visible in the mass projection, Fig. 6. In regard to this, an angular

analysis is needed to separate different contributions. The contributing amplitudes are parametrized using nonrelativistic Zemach tensor formalism [7, 8], the four-body amplitude analysis allows to determine the fractions and the phases of contributing resonances.

The analysis strategy can be separated into three stages:

- As a first approach, the resonance (R^0) lineshape is described by a complex relativistic Breit-Wigner function.
- Second approach; the resonance amplitudes are described by a quasi-model-independent method (QMI).
- The mixing between $J^P = 1^+$ amplitudes is allowed.

In the first and second part of the strategy, it is taken into account that the mass term of some amplitudes not always are well described by Breit-Wigner functions. One explanation is that resonances are broad or because they populate high mass regions. In this sense, for a given J^P, a QMI method is tested to describe an amplitude while leaving the other resonances parametrized with Bret-Wigner functions. The QMI amplitudes are introduced one by one, with free parameters being the real and imaginary part of the amplitudes in each bin of the $D^{*+}\pi^-$ spectrum. The reference resonance is usually taken as 1^+D. When the QMI parameters are found, a second iteration is performed using as input the fitted solution. The initial values of each free parameters have random values. The QMI fit starts with the $J^P = 1^+S$ amplitude, once the solution has been determined, it is fixed and a QMI analysis of $J^P = 0^-$ is performed. Continuing with the procedure, the $J^P = 0^-$ amplitude is fixed and the Breit-Wigner parameters of all tested resonances are let to free to float in the one by one. This procedure is repeated iteratively until the process converges and no significant variation of the free parameters is observed. Parameters values as results [6] of this process can be seen in the first part of Table 2.

Resonance	J^P	Mass [MeV]	Width [MeV]	Significance (σ)
$D_1(2420)$	1^+	$2424.8 \pm 0.1 \pm 0.7$	$33.6 \pm 0.3 \pm 2.7$	
$D_1(2430)$	1^+	$2411 \pm 3 \pm 9$	$309 \pm 9 \pm 28$	
$D_2^*(2460)$	2^+	2460.56 ± 0.35	47.5 ± 1.1	
$D_0(2550)$	0^-	$2518 \pm 2 \pm 7$	$199 \pm 5 \pm 17$	53
$D_1^*(2600)$	1^-	$2641.9 \pm 1.8 \pm 4.5$	$149 \pm 4 \pm 20$	60
$D_2(2740)$	2^-	$2751 \pm 3 \pm 7$	$102 \pm 6 \pm 26$	16
$D_3^*(2750)$	3^-	$2753 \pm 4 \pm 6$	$66 \pm 10 \pm 14$	8.7
D_1	1^+	$2423.7 \pm 0.1 \pm 0.8$	$31.5 \pm 0.1 \pm 2.1$	
D_1'	1^+	$2452 \pm 4 \pm 15$	$444 \pm 11 \pm 36$	

Table 2: Resonance parameters from amplitude analysis. The first part shows the results from the amplitude analysis, the second part from a mixing analysis. First uncertainty is statistical and second systematic.

Exploring the fitted magnitude and phase of the 1^+S amplitude, a broad structure near the threshold was found. This is shown in Fig. 7. From the phase motion plot, in the 2.8 GeV region mass, it can be seen that this structure behave as a resonance, suggesting an additional 1^+S

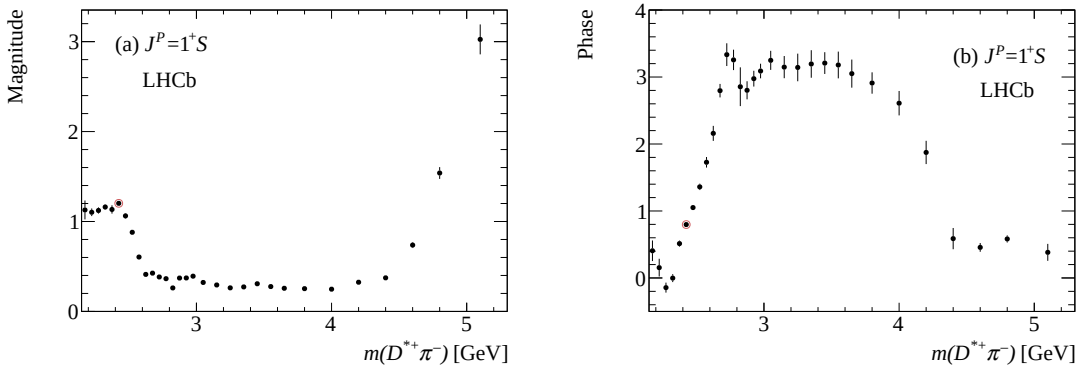

Figure 7: *a*) Magnitud and *b*) phase of the 1^+S amplitude from the QMI method.

contribution. Nevertheless when included in the fit with free parameters no significant contribution was obtained.

The amplitude and phase for the $J^P = 0^-$ QMI are shown in Fig. 8. Besides the presence of the $D_0(2550)$ resonance, activity can be seen around 2,8 GeV mass consistent with a resonance (a new $D_0^{'}$ resonance). From the fit the following parameters are obtained

$$m(D_0^{'}) = 2782 \pm 13 \text{ MeV} \qquad \Sigma(D_0^{'}) = 146 \pm 23 \text{ MeV},$$

with 3.2σ significance. However, when included in the amplitude analysis, its relative contribution is very small. The results from the QMI model can be seen in Table 3

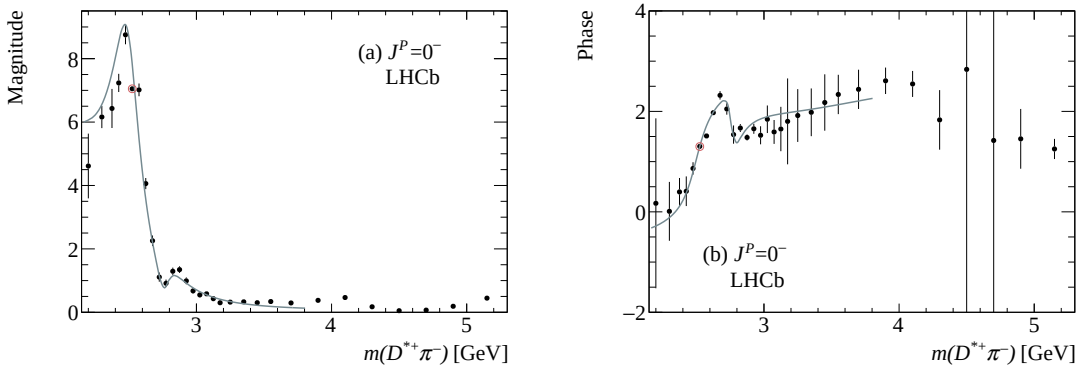

Figure 8: *a*) Magnitud and *b*) phase of the $J^P = 0^-$ amplitude from the QMI method.

The search for additional contributions was also tested. No evidence for $D_1^*(2760)$ or $D_2^*(3000)$ previously observed in $B^- \to D^+\pi^-\pi^-$ [] was found. Their statistical significance is reported to be of 2.4 and 0.0 respectively. The data is also fitted allowing for a mixing between D_1 and $D_1^{'}$ resonances. The mixing angle deviates from zero by 2.3σ.

Resonance	J^P	fraction (%)	phase (rad)
$D_1(2420)$	1^+D	$59.8 \pm 0.3 \pm 2.9$	0
1^+S QMI	1^+S	$28.3 \pm 0.3 \pm 1.9$	$-1.19 \pm 0.01 \pm 0.15$
$D_2^*(2460)$	2^+	$15.3 \pm 0.2 \pm 0.3$	$-0.71 \pm 0.01 \pm 0.48$
$D_1(2420)$	1^+S	$2.8 \pm 0.2 \pm 0.5$	$1.43 \pm 0.02 \pm 0.31$
0^- QMI	0^-	$10.6 \pm 0.2 \pm 0.7$	$1.94 \pm 0.01 \pm 0.19$
$D_1^*(2600)$	1^-	$6.0 \pm 0.1 \pm 0.6$	$1.20 \pm 0.02 \pm 0.05$
$D_2(2740)$	2^-P	$1.9 \pm 0.1 \pm 0.4$	$-1.57 \pm 0.04 \pm 0.15$
$D_2(2740)$	2^-F	$3.2 \pm 0.2 \pm 1.1$	$1.11 \pm 0.04 \pm 0.29$
$D_3^*(2750)$	3^-	$0.35 \pm 0.04 \pm 0.05$	$-1.17 \pm 0.07 \pm 0.31$
Sum		$128.2 \pm 0.6 \pm 3.8$	

Table 3: Amplitude analysis results with $J^P = 1^+S$ and $J^P = 0^-$ amplitudes described by QMI.

3. Amplitude analysis of $B^+ \to D^+D^-K^+$ decays and model-independent analysis of $B^+ \to D^+D^-K^+$

The family of decays $B^+ \to D^{(*)+}D^{(*)}K^+$ offers a good laboratory to study charmonium states. Branching fractions measurements have been performed [9–11] but not prior analysis to their resonant structure exits. Particularly, $B^+ \to D^+D^-K^+$ provides a clean environment to perform studies. For example, resonances in the D^-K^+ system are expected to have minimum quark content ($\bar{c}d\bar{s}u$), thus any indication of resonance content would be exotic. On the other hand, conventional resonances can only contribute in the D^+D^- channel. With unprecedented pure sample obtained by the LHCb experiment, corresponding to an integrated luminosity of 9 fb^{-1}, the first $B^+ \to D^+D^-K^+$ amplitude analysis is presented. Also, a model-independent analysis is performed to study the resonant structures in the D^+D^- channel.

The B meson reconstructed as $B^+ \to (K^-\pi^+\pi^+)_{D^+}(K^+\pi^-\pi^-)_{D^-}K^+$ is filtered through a selection criteria in order to separate signal from background events. From a maximum likelihood fit, a total of 1374 candidates are extracted. Within a signal window of 40 MeV/c^2 around the B mass, 1260 candidates are obtained with a purity greater thant 99.5%. The projection of signal events in the Dalitz plot can be seen in Fig. 9. Projections are also shown. From the plot at the bottom left, Fig. 9 *c*), a clear excess is observed at a mass around 8.25 GeV$^2/c^4$.

Two strategies are followed in this study [12]. In the first one, the total signal amplitude is constructed only including charmonium resonance in D^+D^-. It is expected natural J^P to pseudoscalars and suppression of high-spin contributions. The components included in the model are shown in Table 4. The possibility if a spin-0 contribution to $\chi_{c2}(3930)$ was not excluded. The mass and width of $\psi(3770)$, $\psi(4040)$, $\psi(4160)$ and $\psi(4415)$ are allowed to float and an exponential S-wave is included in the D^-K^+ system describing the nonresonant component. The results show a clear disagreement between the model and data at the region around $m(D^-K^+) \sim 2.9$ GeV/c^2 as seen in Fig. 10.

In the second strategy, the baseline model is constructed adding D^-K^+ resonances. The best fit was obtained including spin-0 and spin-1 D^-K^+ contributions which are labeled as $\chi_0(2900)$ and $\chi_1(2900)$. Nonetheless is not excluded the possibility that hadronic effects, such as rescattering could also explain the best agreement with data. For this last hypothesis more data is needed. In the

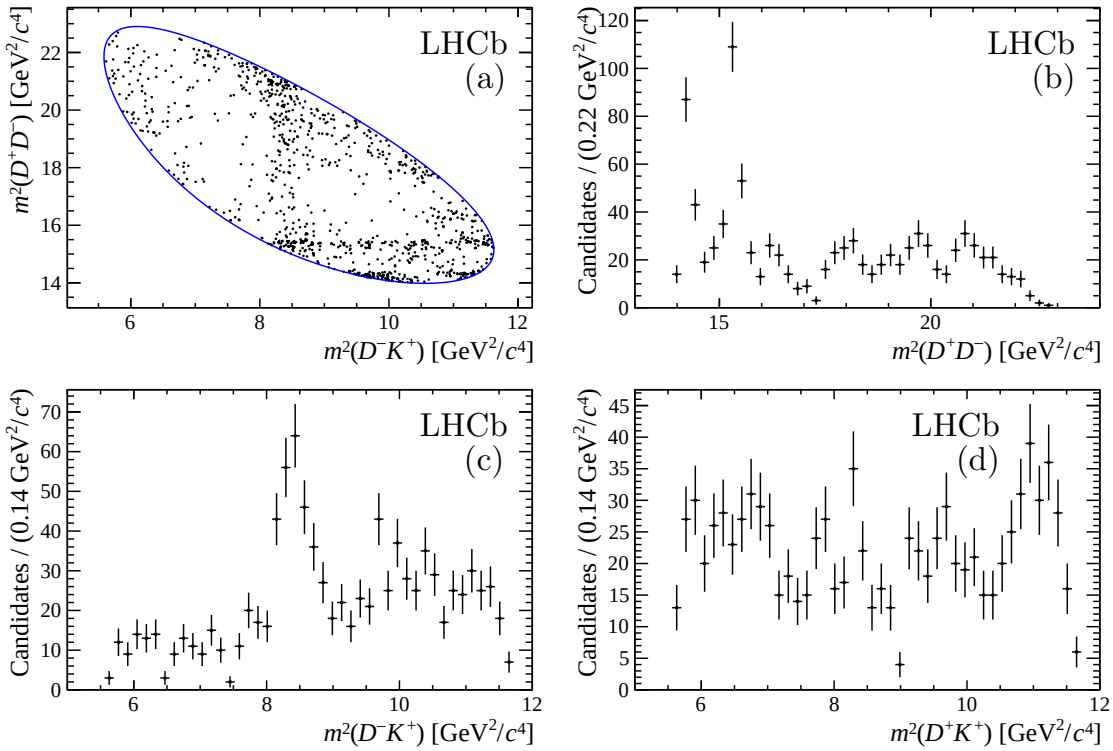

Figure 9: Run II Signal candidates entering in the the Dalitz plot fit projected in the phase space as well as in each system.

Partial wave (J^{PC})	Resonance	Mass (MeV/c^2)	Width (MeV)
S wave (0^{++})	$\chi_{c0}(3860)$	3862 ± 43	201 ± 145
	$X(3915)$	3918.4 ± 1.9	20 ± 5
P wave (1^{--})	$\psi(3770)$	3778.1 ± 0.9	27.2 ± 1.0
	$\psi(4040)$	4039 ± 1	80 ± 10
	$\psi(4160)$	4191 ± 5	70 ± 10
	$\psi(4260)$	4230 ± 8	55 ± 19
	$\psi(4415)$	4421 ± 4	62 ± 20
D wave (2^{++})	$\chi_{c2}(3930)$	3921.9 ± 0.6	36.6 ± 2.1
F wave (3^{--})	$X(3842)$	3842.71 ± 0.20	2.79 ± 0.62

Table 4: Components included in the Dalitz plot fit following strategy I.

$D\bar{D}$ system, structure at the $\chi_{cJ}(3930)$ region, is found to be best described by spin-0 and spin-2 contributions. The Baseline model is shown in Table 5 and 6. The projection of the model overlaid with data is shown in Fig. 11.

Using a model-independent analysis, these results are reinforced [13]. The distribution of the cosine of D^+D^- helicity angle expressed in terms of Legendre Polynomials is considered to perform a coefficient expansion, the k-th unnormalised moments. Decomposition in slice of $m(D^+D^-)$ is taken into account and the several hypothesis are tested. Results shows that indeed an $X_0(2900)$ and

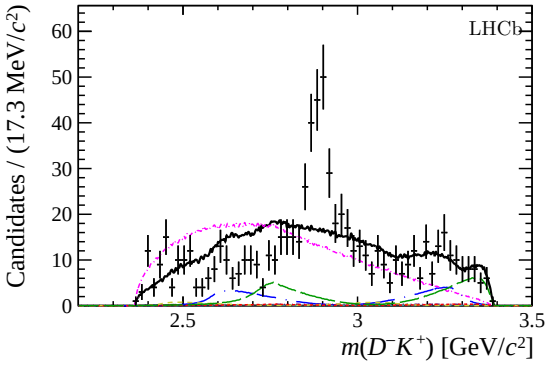

Figure 10: Projection of the Dalitz plot fit and individual model components in the D^-K^+ channel. Data is shown in black.

Resonance	Magnitude	Phase (rad)	Fit fraction (%)
D^+D^- resonances			
$\psi(3770)$	1 (fixed)	0 (fixed)	$14.5 \pm 1.2 \pm 0.8$
$\chi_{c0}(3930)$	$0.51 \pm 0.06 \pm 0.02$	$2.16 \pm 0.18 \pm 0.03$	$3.7 \pm 0.9 \pm 0.2$
$\chi_{c2}(3930)$	$0.70 \pm 0.06 \pm 0.01$	$0.83 \pm 0.17 \pm 0.13$	$7.2 \pm 1.2 \pm 0.3$
$\psi(4040)$	$0.59 \pm 0.08 \pm 0.04$	$1.42 \pm 0.18 \pm 0.08$	$5.0 \pm 1.3 \pm 0.4$
$\psi(4160)$	$0.67 \pm 0.08 \pm 0.05$	$0.90 \pm 0.23 \pm 0.09$	$6.6 \pm 1.5 \pm 1.2$
$\psi(4415)$	$0.80 \pm 0.08 \pm 0.06$	$-1.46 \pm 0.20 \pm 0.09$	$9.2 \pm 1.4 \pm 1.5$
D^-K^+ resonances			
$X_0(2900)$	$0.62 \pm 0.08 \pm 0.03$	$1.09 \pm 0.19 \pm 0.10$	$5.6 \pm 1.4 \pm 0.5$
$X_1(2900)$	$1.45 \pm 0.09 \pm 0.03$	$0.37 \pm 0.10 \pm 0.05$	$30.6 \pm 2.4 \pm 2.1$
Nonresonant	$1.29 \pm 0.09 \pm 0.04$	$-2.41 \pm 0.12 \pm 0.51$	$24.2 \pm 2.2 \pm 0.5$

Table 5: Baseline model following strategy II.

Resonance	Mass (GeV/c^2)	Width (MeV)
$\chi_{c0}(3930)$	$3.9238 \pm 0.0015 \pm 0.0004$	$17.4 \pm 5.1 \pm 0.8$
$\chi_{c2}(3930)$	$3.9268 \pm 0.0024 \pm 0.0008$	$34.2 \pm 6.6 \pm 1.1$
$X_0(2900)$	$2.866 \pm 0.007 \pm 0.002$	$57 \pm 12 \pm 4$
$X_1(2900)$	$2.904 \pm 0.005 \pm 0.001$	$110 \pm 11 \pm 4$

Table 6: Parameters for the $\chi_{c0,2}(3930)$ and $X_{0,1}(2900)$ resonances from the fit.

$X_1(2900)$ are needed in the D^-K^+ channel. This constitute the first observation of exoctic hadron with open flavor. The hypothesis of including both spi-0 and spin-2 states in the $\chi_{cJ}(3930)$ region is also favored [13].

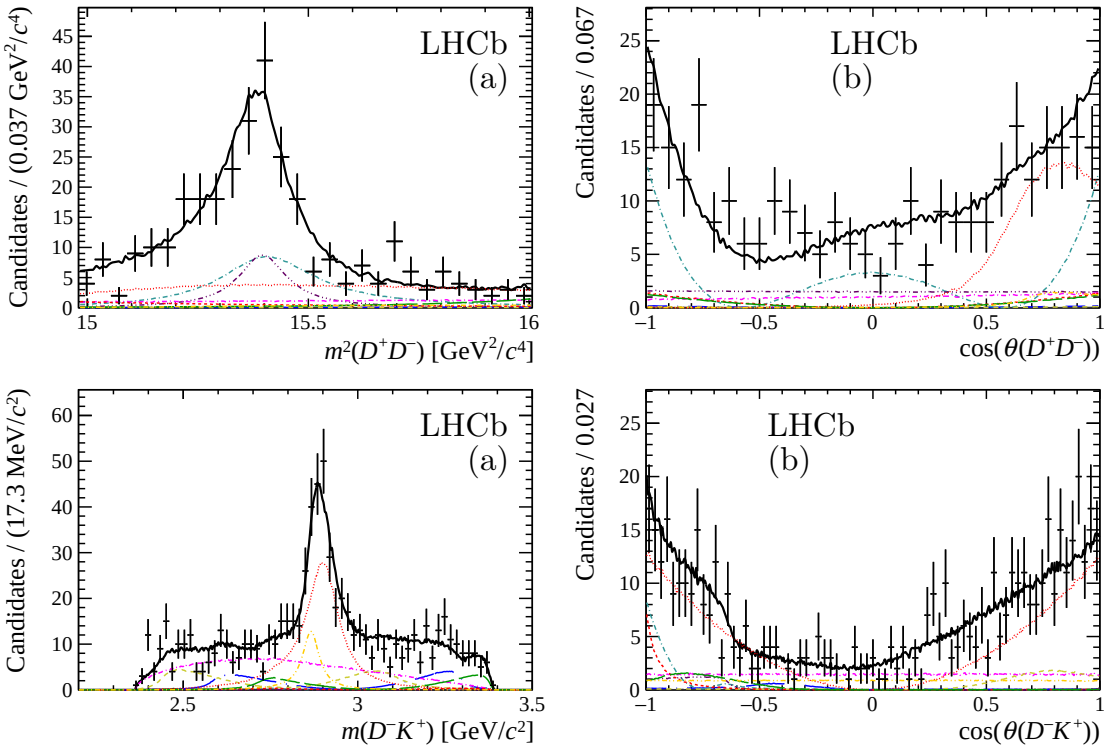

Figure 11: Projection on the D^-K^+ channel (first row) and $D+D^-$ channel (second row). The cosine of the helicity angle is shown for each system.

References

[1] S. Godfrey and K. Moats, *Properties of excited charm and charm-strang mesons*. Phys. Rev. D93, 034035 (2016).

[2] T. Barnesm F. E. Close, and H. J. Lipkin, *Implications of a DK molecule at 2.32 GeV,*. Phys. Lett B578, (2004) 365.

[3] Particle Data Group, P. A. Zyla and others, *Review of particle physics*. `http://pdg.lbl.gov/`, Prog. Theor. Exp. Phys. 2020 (2020) 083C01.

[4] T. Skwarnicki, *A study of the radiative cascade transitions between the Upsilon-prime and Upsilon resonances*. PhD thesis, Institute of Nuclear Physics, Krakow, 1986.

[5] LHCb collaboration R. Aaij and others, *Observation of a new D_s^+ meson in $B^0 \to D^-D^+K^+\pi^-$ decays*. Phys. Lett 126, (2021) 122002.

[6] LHCb collaboration R. Aaij and others, *Determination of quantum numbers for several excited charmed mesons observed in $B^- \to D^{*+}\pi^-\pi^-$*. Phys. Lett D101, (2020) 032005.

[7] C. Zemach, *Three pion decays of unstable particles*. Phys. Rev 133, (1964) B1201.

[8] V. Filippini, *Covariant spin tensors in meson spectroscopy*. Phys. Rev D51, (1995) 2247.

[9] BaBar collaboration, P. del Amo Sanchez et al, *Measurement of the $B \to \bar{D}^{(*)}D^{(*)}K$ branching fractions*. Phys. Rev D83, (2011) 032004.

[10] Belle collaboration, J. Brodzicka et al, *Observation of a new D_{sJ} meson in $B^+ \to \bar{D}^0 D^0 K^+$ decays*. Phys. Rev Lett.100, (2008) 092001.

[11] LHCb collaboration R. Aaij and others, *First observation of the decay $B^+ \to D^0 \bar{D}^0 K^+ \pi^-$* . Phys. Rev D102, (2020) 051102.

[12] LHCb collaboration R. Aaij and others, *Amplitude analysis of $B^+ \to D^+ D^- K^+$ decays* . Phys. Rev D101, (2020) 032005.

[13] LHCb collaboration R. Aaij and others, *Model-independent studies of $B^+ \to D^+ D^- K^+$ decays*. Phys. Rev D102, (2020) 112003.